metals

MDPI

Article

The Efficient Removal of Calcium and Magnesium Ions from Industrial Manganese Sulfate Solution through the Integrated Application of Concentrated Sulfuric Acid and Ethanol

Houyang Chen [1,†], Kaituo Wang [1,2,*,†], Xianquan Ming [3], Feng Zhan [3,*], Yaseen Muhammad [4], Yuezhou Wei [1], Weijian Li [3] and Haiqing Zhan [3]

1 Guangxi Key Laboratory of Processing for Non-Ferrous Metals and Featured Materials, School of Resources, Environment and Materials, Guangxi University, Nanning 530004, China; chy937659953@163.com (H.C.); yzwei@gxu.edu.cn (Y.W.)
2 MOE Key Laboratory of New Processing Technology for Nonferrous Metals and Materials, Nanning 530004, China
3 South Manganese Group Co., Ltd., Nanning 530004, China; mxq@southmn.com (X.M.); lwj@southmn.com (W.L.); zhq@southmn.com (H.Z.)
4 Institute of Chemical Sciences, University of Peshawar, Khyber Pakhtunkhwa 25120, Pakistan; myyousafzai@gmail.com
* Correspondence: wangkaituo@gxu.edu.cn (K.W.); phy_ideaa@outlook.com (F.Z.)
† These authors contributed equally to this work.

check for updates

Citation: Chen, H.; Wang, K.; Ming, X.; Zhan, F.; Muhammad, Y.; Wei, Y.; Li, W.; Zhan, H. The Efficient Removal of Calcium and Magnesium Ions from Industrial Manganese Sulfate Solution through the Integrated Application of Concentrated Sulfuric Acid and Ethanol. *Metals* **2021**, *11*, 1339. https://doi.org/10.3390/met11091339

Academic Editors: Jean François Blais and Srecko Stopic

Received: 17 June 2021
Accepted: 23 August 2021
Published: 25 August 2021

Abstract: In the process of preparing high-purity $MnSO_4$ from industrial $MnSO_4$ solution, it is difficult to remove Ca^{2+} and Mg^{2+} due to their closely similar properties. In this study, thermodynamic software simulation and experimental procedures were combined to remove Ca^{2+} and Mg^{2+} from industrial $MnSO_4$ solution to obtain high-purity $MnSO_4$. The simulation model was applied to predict the trend of the crystallization of different ions in the solution upon the addition of H_2SO_4, which revealed that, at a volume ratio of H_2SO_4 to $MnSO_4$ solution of more than 0.2, $MnSO_4$ started to crystallize and precipitate. The experimental results further verified the simulation results, and the yield of $MnSO_4$ increased with the increasing ratio of H_2SO_4, while the removal rate of Ca^{2+} and Mg^{2+} decreased gradually. Keeping the economic aspect in mind, the 0.3 ratio of H_2SO_4 was selected at which the yield of $MnSO_4$ reached 86.44%. The removal rate of Ca^{2+} and Mg^{2+} by recrystallization reached 99.68% and 99.17% respectively after six consecutive cycles. The recrystallized sample was washed twice with anhydrous ethanol (volume ratio of ethanol to $MnSO_4$ solution of 0.5) and dried for 6 h at 120 °C, and the purity of $MnSO_4 \cdot H_2O$ reached the battery grade requirements with the final yield as high as 80.54%. This study provides important guideline information for the purification of $MnSO_4 \cdot H_2O$ from industrial $MnSO_4$ solution via a cost-effective, simple and facile approach.

Keywords: OLI Stream Analyzer; high-purity $MnSO_4$; recrystallization; Ca^{2+} and Mg^{2+} removal

1. Introduction

$MnSO_4$, as a base manganese salt, is used in the preparation of various advanced manganese-based alloys and products [1–4]. The front drive system of the positive triumvirate of a battery's material (Ni-Cobalt Manganese Acid Lithium) requires high-purity $MnSO_4$, where the major impurities include potassium, sodium, calcium and magnesium (the sum of the concentration of calcium and magnesium impurities is $\leq$0.05%) [5,6]. In order to obtain these high-quality manganese-based materials for use in batteries, the purity of manganese-based raw materials must be solved first. Therefore, the deep decontamination of $MnSO_4$ solution for producing high-grade materials to be used in lithium-ion batteries has become a research hotspot [7].

Among the many impurities like K^+, Na^+, Ca^{2+} and Mg^{2+}, the chemical properties of manganese are closely similar to the calcium and magnesium present in $MnSO_4$ solu-

tion, and hence it becomes very tough to prepare $MnSO_4$ for meeting the requirements of high-purity $MnSO_4$ via traditional decontamination methods [8,9]. In addition, Ca^{2+} and Mg^{2+} have a great impact on many subsequent processes, and in the electrolytic manganese phase, they affect the current efficiency of electrolysis and the purity of electrolytic manganese products. The traditional methods for the removal of Ca^{2+} and Mg^{2+} in $MnSO_4$ solution mainly include chemical precipitation [10,11], recrystallization [12,13], fluoridation [14], extraction [15–17], and electrolysis [18]. Recrystallization includes evaporative concentration, high temperature and pressure crystallization [19–21], where it uses $MnSO_4$ solubility, which shows a sharp decrease at temperatures of over 100 °C, and the $MnSO_4$ crystals are obtained by heating the solution in the high-pressure reactor. This process is very stringent on the material and quality requirements of the equipment, otherwise it can affect the normal safe operation of the system [22,23]. The fluoride method uses the difference between the solubilities between manganese fluoride, calcium fluoride and magnesium fluoride, and the decontamination of Ca^{2+} and Mg^{2+} [24]. However, this method introduces Na^+, NH_4^+ and F^- as impurities while removing Ca^{2+} and Mg^{2+}, and high-purity $MnSO_4$ needs to be treated with extractors and adsorbents for their removal. In addition, the waste liquid and residue produced by this process contains hazardous F^- which requires further purification processes. The extraction method utilizes the difference in solubilities of Mn^{2+} and the impurity ions (K^+, Na^+, Ca^{2+} and Mg^{2+}) in different extractants for effective separation [25], but the product purity and recovery rate obtained by this method is low. Electrolysis uses the difference in the rate of precipitation of manganese ions and impurity ions in manganese sulfate leaching solution, though it generates hydrogen, which poses a safety hazard.

In view of the aforementioned shortcomings of traditional $MnSO_4$ purification processes, and to maintain the sustainable exploitation of resources and the perspective of economic development, it is particularly important to study, develop and apply new processes for the generation of high-purity $MnSO_4$. Thus, this study applies the approach of variation in the solubility–product constant (K_{sp}) of Mn^{2+}, and Ca^{2+} and Mg^{2+} in the water–H_2SO_4 system for the preparation of high-purity $MnSO_4 \cdot H_2O$ at room temperature [26,27]. The impurity ions are removed by repeated recrystallization, and the H_2SO_4 remaining on the surface is washed with ethanol, with the high-purity $MnSO_4 \cdot H_2O$ obtained after drying. Compared with the traditional synthesis method, this method is cost- and energy-effective and simplified with reduced mechanical requirements, while maintaining sustainable and green development approaches by effectively utilizing waste and environmentally friendly materials for the production of high-purity $MnSO_4 \cdot H_2O$.

2. Experimental Section

2.1. Materials and Equipment

The concentration of various ions in the $MnSO_4$ leaching solution (CITIC Dameng Mining Industries Limited Chongzuo Branch, Nanning, Guangxi, China) used in this work is shown in Table 1 (pH = 2.8). The H_2SO_4 used in this experiment was obtained from Chengdu Kelong chemical reagent factory, China. Ethanol was provided by Guangdong Guanghua Sci-Tech Co., Ltd., Guangzhou China. The constant-temperature magnetic heating mixer was provided by Gongyi Yuhua Instrument Co., Ltd. Ethanol was recovered via a rotary evaporator (EYELA-1300D-WB, Tokyo Japan), while solution pH was tested via a pH meter provided by Shanghai San-Xin Instrumentation, China.

Table 1. The concentration of ions in the $MnSO_4$ leaching solution (g/L).

Ion	Mn (g/L)	Mg (mg/L)	Ca (mg/L)	Na (mg/L)	K (mg/L)	Ni (mg/L)	Co (mg/L)	Zn (mg/L)
Concentration	139.20 ± 1.24	1726.39 ± 39.51	544.95 ± 8.99	93.11 ± 9.13	23.62 ± 6.91	236.87 ± 6.88	64.20 ± 1.02	48.20 ± 7.94

2.2. Simulation Software and Methods

OLI Stream Analyzer predicted the system phase equilibrium and crystallization thermodynamic process of complex chemical mixtures in aqueous systems. Different pH values, temperature and pressure could be adjusted according to experimental requirements, and the solute saturation point, precipitation point, acid-base titration curve and thermodynamic properties of the components and their dependence relationships could be simulated and predicted. The ratio of H_2SO_4 to the crystallization trend of different components and the change of $MnSO_4 \cdot H_2O$ yield with temperature were calculated by the software OLI Stream Analyzer version 3.1.

2.3. Preparation of High-Purity $MnSO_4 \cdot H_2O$

High-purity $MnSO_4 \cdot H_2O$ was prepared by H_2SO_4 in coordination with ethanol, and this preparation process is shown in Figure 1. Firstly, 50 mL of $MnSO_4$ solution was taken in a beaker at room temperature, and 15 mL of H_2SO_4 was slowly added to it under continuous stirring. When the crystals were completely precipitated, stirring was stopped and the crystals were separated from the solution. The obtained crystals were re-dissolved with 30 mL deionized water, and then 15 mL H_2SO_4 was slowly added to completely precipitate the crystals. This process was repeated 6 times. Secondly, the filtered $MnSO_4$ crystals were washed with 50 mL of ethanol in two steps to remove H_2SO_4 on the surface, and ethanol was recycled through the rotary evaporator. Finally, the $MnSO_4$ crystals were dried at 120 °C for 6 h to obtain high-purity $MnSO_4 \cdot H_2O$.

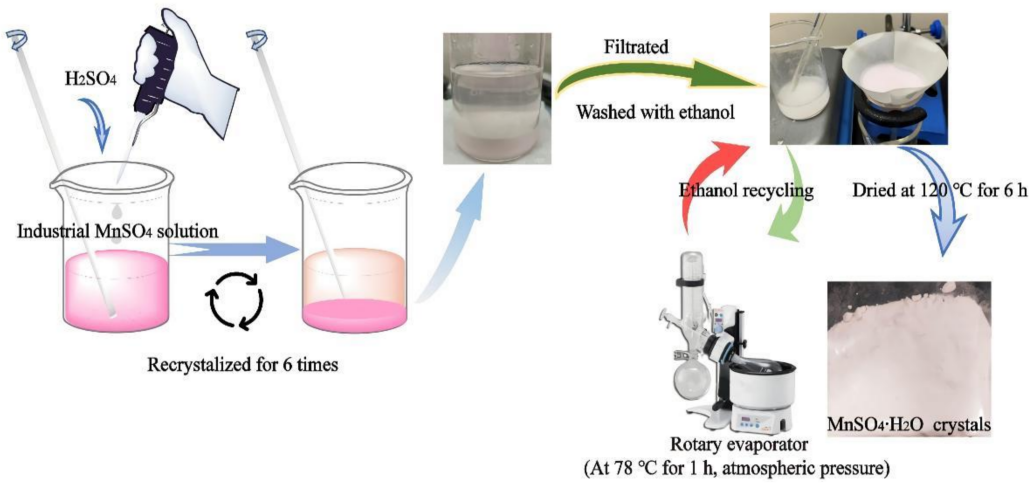

Figure 1. Preparation flow chart of $MnSO_4 \cdot H_2O$ crystals.

2.4. Characterization

X-ray powder diffraction (XRD, Rigaku MiniFlex 600, Japan) was used to analyze the crystal phase structure of $MnSO_4 \cdot H_2O$ in scanning range of 10–70° (2θ) at a rate of 5°/min under Fe-Kα as anode target, 40 kV and 15 mA conditions. The sample was digested with 5% HCl. The concentrations of various metal ions in manganese sulphate leaching solution and filtrate were measured by inductively coupled plasma atomic emission spectroscopy (ICPS-7510, Shimadzu, Japan) and atomic absorption spectrophotometer (AA-7000, Shimadzu, Japan), respectively.

3. Results and Discussions

3.1. Simulation Results of OLI Stream Analyzer Software

The density of the industrial $MnSO_4$ solution used in this experiment was 1.3127 ± 0.0004 g/cm^3, and the density calculated by the OLI Stream Analyzer software was 1.2982 g/cm^3, hence it could be concluded that the OLI Stream Analyzer software could be used to simulate and calculate the industrial $MnSO_4$ solution. The software was used to calculate the scaling trend and yield changes of different components of industrial

$MnSO_4$ solution with the addition ratio of H_2SO_4. As shown in Figure 2A, the scaling trend of $MnSO_4 \cdot H_2O$, $CaSO_4$ and $MgSO_4 \cdot H_2O$ increased with the increasing ratio of H_2SO_4. When the ratio of H_2SO_4 reached 6% and 10%, the scaling trend of $MnSO_4 \cdot H_2O$ and $CaSO_4$ in the solution reached 1 [28], which indicated that $MnSO_4 \cdot H_2O$ and $CaSO_4$ were saturated and had reached the precipitation condition. In contrast, the $MgSO_4 \cdot H_2O$ crystal does not match the precipitation condition. In a temperature range of 25–85 °C, the change trend of $MnSO_4 \cdot H_2O$ yield with the ratio of H_2SO_4 is shown in Figure 2B. The yield of $MnSO_4 \cdot H_2O$ increased with the increasing ratio of H_2SO_4, and was sensitive to temperature change when the ratio of H_2SO_4 was less than 26%, the main reason for this was that the solubility of manganese sulfate decreased with the increase of temperature at 25–85 °C, which led to the increase of crystallization yield. However, when the H_2SO_4 concentration was high and the ratio exceeded 26%, the $MnSO_4 \cdot H_2O$ saturation increased. Under the condition of a ratio of 30% H_2SO_4, the solution degree of $MnSO_4 \cdot H_2O$, increased with the increase in temperature, which led to a slight change in the crystallization yield. Therefore, when the ratio of H_2SO_4 was 30%, the maximum yield of $MnSO_4 \cdot H_2O$ was 82.2% at 25 °C.

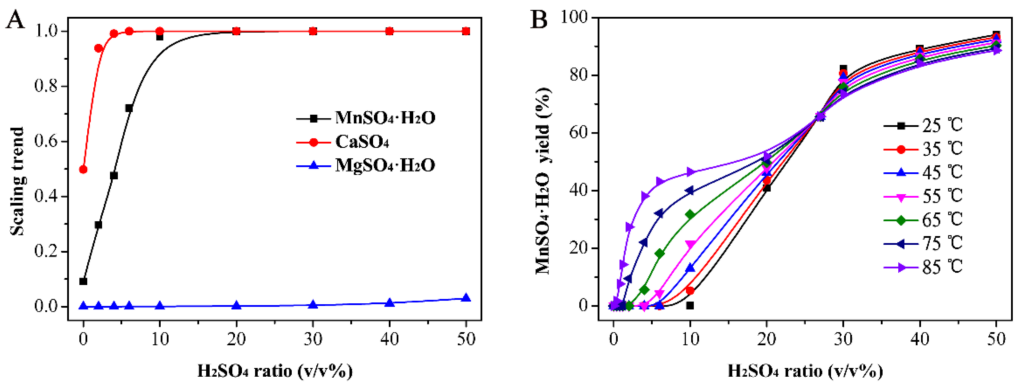

Figure 2. The scaling trend (**A**) of different components of industrial $MnSO_4$ solution with the addition ratio of H_2SO_4 and $MnSO_4 \cdot H_2O$ yield (**B**) in the temperature range of 25–85 °C.

3.2. Calculated and Tested Yield of Different Components

Under the condition of 25 °C, in order to obtain the influence of H_2SO_4 on the yield of different components ($MnSO_4 \cdot H_2O$, $CaSO_4$ and $MgSO_4 \cdot H_2O$), the comparison of the results of the calculations and tests were used to obtain the yield of different components of industrial $MnSO_4$ solution, with the addition of H_2SO_4 in different ratios. As shown in Figure 3, the calculated and tested yield of $MnSO_4 \cdot H_2O$ was very close to the change trend of the ratio of H_2SO_4 and increased proportionally with increasing H_2SO_4 ratio. When the ratio of H_2SO_4 exceeded 30%, its increasing trend was not obvious. The calculated and tested yields were 82.2% and 86.6%, respectively, at a 30% H_2SO_4 ratio. As the ratio of H_2SO_4 increased, a wide gap appeared between the calculated and tested yield of $CaSO_4$, which was mainly because the industrial $MnSO_4$ solution was laden with a high content of salt (the content of $MnSO_4$ exceeds 100 g/L) and the force between the ions was strengthened, which increases the solubility of $CaSO_4$ [19]. Hence, the actual amount of $CaSO_4$ precipitation was minimal, which was beneficial for the removal of Ca^{2+}. $MgSO_4 \cdot H_2O$ precipitation was not generated in the simulation calculation, but $MgSO_4 \cdot H_2O$ crystals were found in the actual test. This was because $MnSO_4$ and $MgSO_4$ in the solution were similar in structure and could form a mixed crystal system [29]. $MgSO_4$ could attach to the solid surface of $MnSO_4 \cdot H_2O$ for the heterogeneous nucleation and in the actual crystallization process.

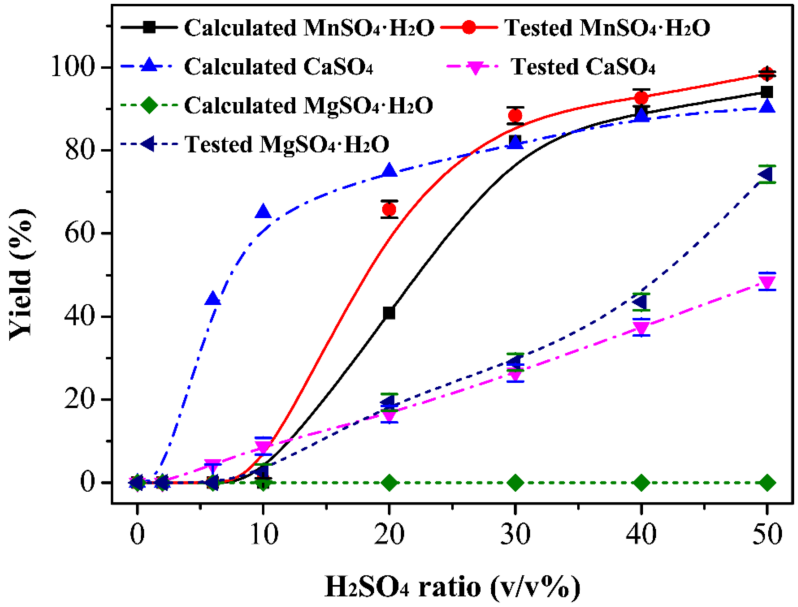

Figure 3. The calculated and tested yield of different components of industrial $MnSO_4$ solution with the addition ratio of H_2SO_4.

3.3. Determination of the Optimal Ratio of H_2SO_4

The change trend of the $MnSO_4 \cdot H_2O$ yield and Ca^{2+}, Mg^{2+} removal rate with the ratio of H_2SO_4 was explored in a range from 20–50%. As shown in Figure 4, the yield of $MnSO_4 \cdot H_2O$ increased with increasing the ratio of H_2SO_4, while the change in the removal rate of Ca^{2+} and Mg^{2+} demonstrated the opposite trend. Considering the actual production cost and the results of the previous calculations, the optimal ratio of H_2SO_4 was determined to be 30% and at this ratio, the $MnSO_4 \cdot H_2O$ crystal yield was 86.60%, and the removal rates of Ca^{2+} and Mg^{2+} were 65.25% and 70.91%, respectively.

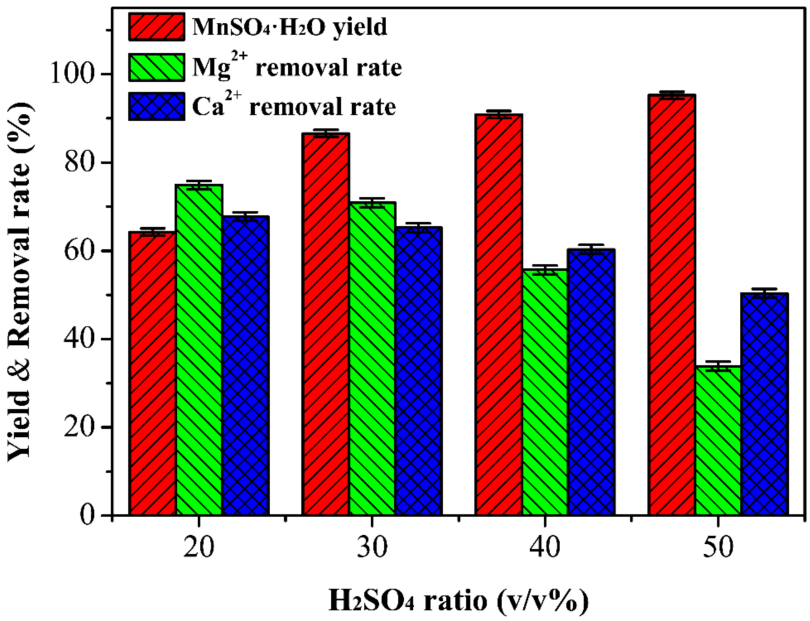

Figure 4. The effect of H_2SO_4 ratio on $MnSO_4 \cdot H_2O$ yield and Mg^{2+}, Ca^{2+} removal rate.

3.4. Recrystallization Experiment

In order to obtain high-purity $MnSO_4 \cdot H_2O$ crystals, it was necessary to perform recrystallization experiments on the obtained $MnSO_4 \cdot H_2O$. The ratio of H_2O and the

number of cycles in the recrystallization process had a great influence on the yield of $MnSO_4 \cdot H_2O$ and the removal rates of Ca^{2+} and Mg^{2+} [30]. The solubility of $MnSO_4$ at 25 °C was around 64.8 g/100 g H_2O [31], and hence the ratio of H_2O added (the volume ratio of H_2O to the original $MnSO_4$ solution) varied between 60–100%. As shown in Figure 5A, the yield of $MnSO_4 \cdot H_2O$ decreased with an increase in the ratio of H_2O which was because the dissolution loss of $MnSO_4$ increased as the amount of water increased, and finally determined that 60% was the optimum ratio of H_2O. It can be seen from Figure 5B that the yield of $MnSO_4 \cdot H_2O$ decreased with the increase of the number of cycles, while the removal rate of Ca^{2+} and Mg^{2+} gradually increased. However, the yield of $MnSO_4 \cdot H_2O$ changed marginally, and still reached 80.54% after six cycles. The residual content (wt.%) of Mg^{2+} and Ca^{2+} in $MgSO_4 \cdot H_2O$ with different recrystallization cycles in Table 2 suggested that Ca^{2+} content attained the requirement ($\leq$0.0050%) after two cycles while Mg^{2+} needed six cycles to attain this requirement. The preparation of high-purity $MnSO_4 \cdot H_2O$ crystals in this paper required a minimum of six cycles. During the experiment, excessive concentrated H_2SO_4 was recovered and used in industry to prepare $MnSO_4$ solution by leaching manganese ore. Therefore, the recycling of H_2SO_4 could effectively save immeasurable production costs. At present, compared with the traditional extraction method, this technology was not only simple in operation, lower in cost, and larger in production scale, but also through preliminary feasibility analysis, the annual economic benefits of using this technology were at least twice that of the traditional technology.

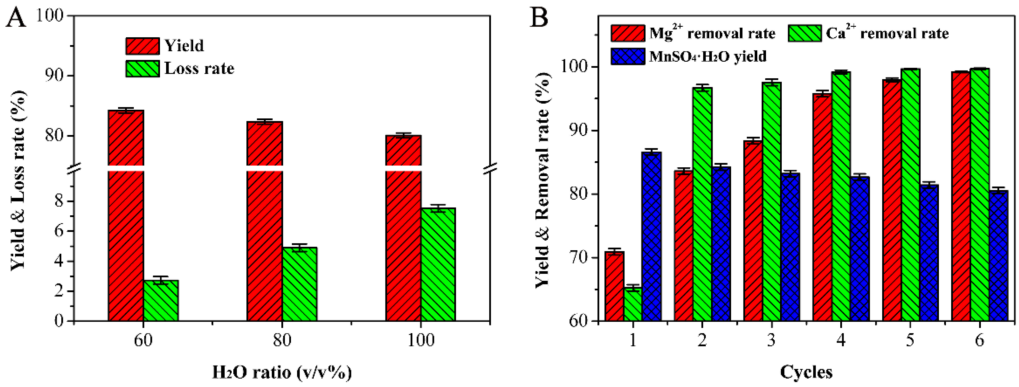

Figure 5. (**A**) The effect of H_2O ratio on $MnSO_4 \bullet H_2O$ yield during recrystallization; (**B**) The effect of cycles on $MnSO_4 \bullet H_2O$ yield and Mg^{2+}, Ca^{2+} removal rate.

Table 2. Residual content (wt.%) of Mg^{2+} and Ca^{2+} in $MnSO_4 \bullet H_2O$ with different recrystallization cycles.

Cycle Number	Mg/wt.%	Ca/wt.%
1	0.11	0.042
2	0.062	0.0040
3	0.044	0.0030
4	0.016	0.0010
5	0.0078	0.00044
6	0.0031	0.00039

3.5. Determination of the Optimal Ratio of Ethanol

The final product obtained in this study were high-purity $MnSO_4 \cdot H_2O$ crystals, which needed to be dried. Figure 6A shows that when the filtered sample was dried at 120 °C for 6 h, the whole sample was still stuck together and there was lot of water on the surface. This was mainly because the system contained a large amount of H_2SO_4 covering the surface of the filtered sample, while its strong water absorption properties made it difficult to remove the water from the sample. The study found that the solubility of $MnSO_4 \cdot H_2O$

in ethanol was very small [32]. Therefore, ethanol was used to clean the H_2SO_4 covering the surface of the sample to obtain a dry sample, and part of the $MgSO_4$ impurity could be removed during the washing process. It can be seen from Figure 6B–F that the sample gradually became loose and dry as the ratio of ethanol increased (the volume ratio of ethanol to the original $MnSO_4$ solution). The sample gradually became loose and dry, and at 100% volume ratio of ethanol, loose and dry $MnSO_4 \cdot H_2O$ crystals were obtained. Figure 7A shows that the yield of $MnSO_4 \cdot H_2O$ crystals gradually decreased as the ratio of ethanol increased, which was because the increase in the ratio of ethanol led to an increase in dissolved $MnSO_4$ [33]. In addition, the $MnSO_4$ samples obtained with different ethanol ratios were placed in a laboratory environment, and the water absorption rate was explored to confirm the complete removal of H_2SO_4. As shown in Figure 7B, the water absorption rate of $MnSO_4$ samples obtained with different ethanol ratios increased with time while that of $MnSO_4 \cdot H_2O$ crystals changed little with time at an ethanol ratio of 100% and 120%, respectively which proved that H_2SO_4 had been successfully removed. From these experiments, a 100% ethanol ratio was selected as the optimum value.

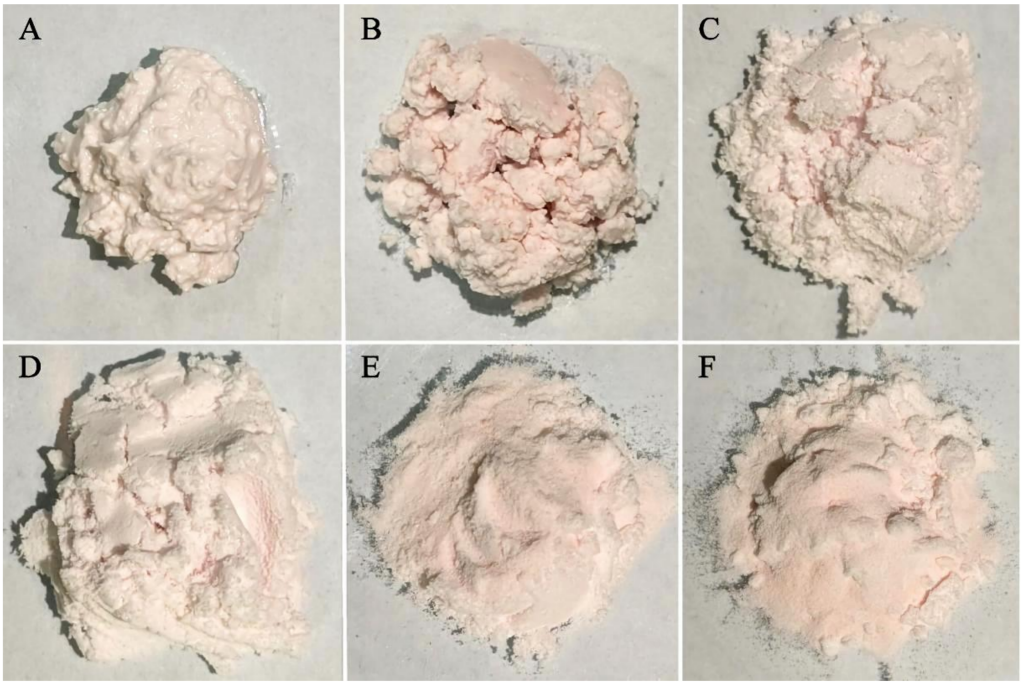

Figure 6. Sample photos of $MnSO_4 \bullet H_2O$ after washing with different ethanol ratios: 0% (**A**), 40% (**B**), 60% (**C**), 80% (**D**), 100% (**E**) and 120% (**F**), and drying at 120 °C for 6 h.

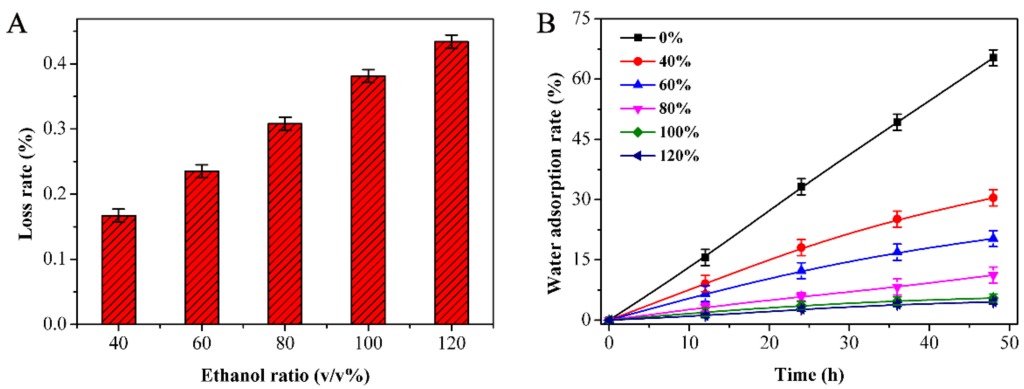

Figure 7. The effect of different ethanol ratios on the loss rate of $MnSO_4 \bullet H_2O$ (**A**) and the water absorption rate of $MnSO_4$ (**B**).

3.6. High-Purity $MnSO_4 \cdot H_2O$ Test Results

The $MnSO_4 \cdot H_2O$ prepared in this study was tested with reference to the HG/T4823-2015 Manganese sulfate for battery materials; the ICP and AAS test results are shown in Table 3. It can be seen that the contents of all of the residual impurity ions had reached the test standards, especially those of Ca^{2+} and Mg^{2} which were 0.002 wt% and 0.004 wt%, respectively, much lower than the test standards. In addition, the pH of the final product at (100 g/L, 25 °C) was 4.0, which was within the range of the standards (4.0–6.5) [4]. Furthermore, the experimental sample and commercial high-purity $MnSO_4 \cdot H_2O$ crystals (99.99%) were analyzed by XRD. Figure 8 shows that the peak shapes of the two crystals were the same and consistent with the standard card (PDF# 81-0018 $MnSO_4 \cdot H_2O$), which further proved that the prepared product consisted of high-purity $MnSO_4 \cdot H_2O$ crystals.

Table 3. Test standards and ICP/AAS results of high-purity $MnSO_4 \bullet H_2O$ crystals.

Inspected Item	Wt.%	
	Standard	Result
$MnSO_4 \cdot H_2O$	≥99	99.3
Mn	≥32	32.3
Fe	≤0.001	0.0005
Zn	≤0.001	0.004
Cu	≤0.001	<0.001
Pb	≤0.001	0.0005
Cd	≤0.0005	0.0001
K	≤0.01	<0.001
Na	≤0.01	0.002
Ca	≤0.01	0.002
Mg	≤0.01	0.004
Ni	≤0.005	<0.001
Co	≤0.005	0.001
insoluble residue	≤0.01	0.007
pH (100 g/L, 25 °C)	4.0–6.5	4.0

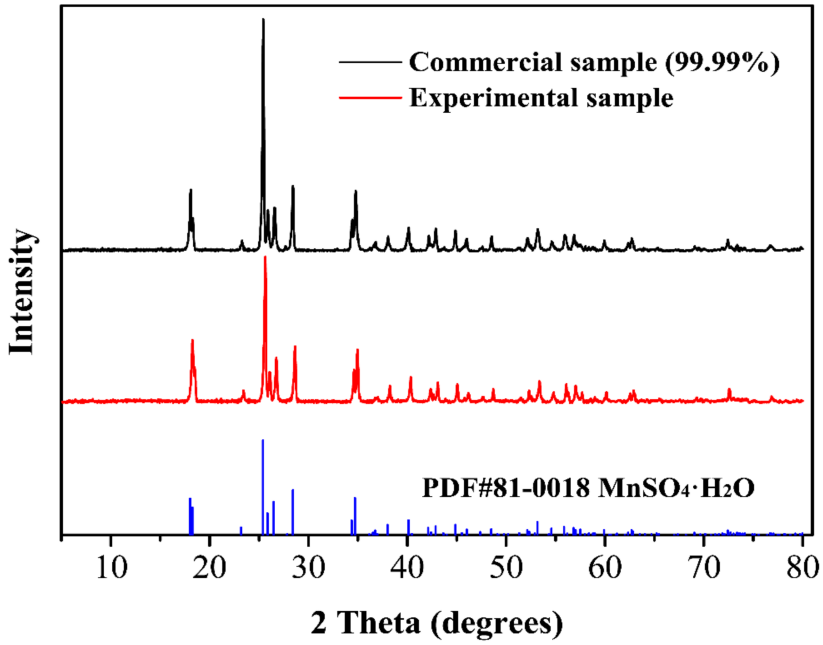

Figure 8. XRD comparison between $MnSO_4 \bullet\bullet H_2O$ crystals obtained in the experiment and commercial high-purity $MnSO_4 \bullet H_2O$ crystals.

4. Conclusions

In this study, the OLI Stream Analyzer software was used to calculate the scaling trend of the industrial $MnSO_4$ solution and the $MnSO_4 \cdot H_2O$ yield at different temperatures with the ratio of H_2SO_4. The scaling trend revealed the reason why Ca^{2+} and Mg^{2+} could be separated. According to the $MnSO_4 \cdot H_2O$ yield at different temperatures, the optimal temperature was determined to be 25 °C. In addition, the ratio of H_2SO_4 was explored through experimental comparative analysis and, combined with factors such as the yield of $MnSO_4 \cdot H_2O$ crystals, the removal rate of Ca^{2+} and Mg^{2+}, and the process cost, it was finally determined that the optimal volume ratio of H_2SO_4 was 30%. The optimal ratio of H_2O in the recrystallization experiment was 60%, which could effectively reduce the loss of $MnSO_4 \cdot H_2O$ crystals and could better remove Ca^{2+} and Mg^{2+}. After six cycles, the removal rates of Ca^{2+} and Mg^{2+} were 99.68% and 99.17%, respectively, and the yield of $MnSO_4 \cdot H_2O$ crystals was 80.54%. The product was washed with ethanol, and the best volume ratio of ethanol was 100%. Finally, the product was tested and analyzed by XRD, ICP and AAS, and all the indicators of the sample met the requirements of high-purity $MnSO_4 \cdot H_2O$ crystals. This study not only solved the problems of a low $MnSO_4 \cdot H_2O$ crystals yield and complex processing in the recrystallization process, but also efficiently removed Ca^{2+} and Mg^{2+}, which could be of great help in practical applications on the industrial-level production of high-purity $MnSO_4 \cdot H_2O$.

Author Contributions: Conceptualization, H.C. and K.W.; methodology, H.C. and Y.W.; software, H.C.; validation, F.Z.; formal analysis, H.C.; investigation, X.M., F.Z., W.L. and H.Z.; resources, K.W. and Y.W.; data curation, H.C.; writing—original draft preparation, H.C. and F.Z.; writing—review and editing, K.W. and Y.M.; visualization, H.C.; supervision, Y.W., W.L. and H.Z.; project administration, K.W. and X.M.; funding acquisition, K.W and F.Z. All authors have read and agreed to the published version of the manuscript. Please turn to the CRediT taxonomy for the term explanation. Authorship must be limited to those who have contributed substantially to the work reported.

Funding: This research was funded by the Science and Technology Major Project of Guangxi Province, grant number: AA18118052. Check carefully that the details given are accurate and use the standard spelling of funding agency names at https://search.crossref.org/funding. Date of access: 24 August 2021. Any errors may affect your future funding.

Institutional Review Board Statement: Not applicable.

Informed Consent Statement: Not applicable.

Data Availability Statement: Not applicable.

Acknowledgments: This work was financially supported by the Science and Technology Major Project of Guangxi Province (AA18118052). The author is very grateful for the funding of the above institutions, thanks to the support and help of the OLI system in the simulation calculation, and thanks to the CITIC Dameng Mining Industries Limited-Guangxi University Joint Research Institute of manganese resources utilization and advanced materials technology, Guangxi University-CITIC Dameng Mining Industries Limited Joint base of postgraduate cultivation for their assistance in the experiment.

Conflicts of Interest: The authors declare no conflict of interest.

References

1. Fan, Y.; Makhlouf, M. Stabilizing the strengthening precipitates in aluminum-manganese alloys by the addition of tungsten. *Mater. Sci. Eng. A* **2017**, *691*, 1–7. [CrossRef]
2. Zhang, D.; Ma, Z.; Spasova, M.; Yelsukova, A.E.; Lu, S.; Farle, M.; Wiedwald, U.; Gökce, B. Formation Mechanism of Laser-Synthesized Iron-Manganese Alloy Nanoparticles, Manganese Oxide Nanosheets and Nanofibers. *Part. Part. Syst. Charact.* **2017**, *34*, 1600225. [CrossRef]
3. Tan, L.; Hu, H.; Liao, J.; Wang, C.; Li, C. Preparation of High-purity Manganese Sulfate for Battery by Solvent Extraction. *Nonferrous Met. (Extr. Metall.)* **2014**, *9*, 62–65. [CrossRef]
4. Zhang, H.; Zhao, K.; Chen, F.; Jiang, Q. Application Prospect and Development of High Pure Manganese Sulfate Monohydrate in Battery Level. *China's Manganese Ind.* **2014**, *32*, 6–8. [CrossRef]

5. Xie, Y.; Ou, Y.; Hu, B.; Ling, Z. Study on production process for high-purity manganese sulfate with waste sulphuric acid of titanium white-pyrolusite-pyrite. *Inorg. Chem. Ind.* **2013**, *45*, 49–51. [CrossRef]
6. Zhao, Y.; Wu, R.; Hu, P.; Jiang, Y.; Jiang, Y. Study on Impurity Characteristics and Purification Process in High Purity Manganese Sulfate. *World Nonferrous Metals* **2020**, 186–188. [CrossRef]
7. Lin, Q.; Liu, Y.; Li, L.; Wang, Y.; Wang, J.; Xu, J.; Si, H.; Peng, B.; Zhu, Z. Study on the process of preparing high-purity manganese sulfate from low-grade manganese carbonate ore. *Inorg. Chem. Ind.* **2014**, *46*, 35–38.
8. Wang, Y.; Wang, W.; Liu, Y.; Liu, F.; Chen, X. Removal of Heavy Metals from manganese sulfate solution and preparation of Battery-level manganese sulfate. *Nonferrous Metals* **2020**, 79–84. [CrossRef]
9. Bao, X.; Wang, Z.; Liu, J.; Su, Z.; Tian, S.; Zhou, D.; Wang, H. Experimental study on the removal of calcium, magnesium and iron from the depth of industrial manganese sulfate. *Min. Metall. Eng.* **2013**, *33*, 90–93. [CrossRef]
10. Xie, Y.; Ye, Y.; Xie, X.; Nong, Y. Removal of Calcium and Magnesium from Manganese Sulfate by Manganese Fluoride. *Technol. Dev. Chem. Ind.* **2020**, *49*, 9–11. [CrossRef]
11. He, T.; Qian, L.; Cui, J.; Shu, H. Deep Removal of Ca and Mg from Industrial Manganese Sulfate with Fluorination Precipitation. *Nonferrous Met. (Extr. Metall.)* **2018**, 5–8. [CrossRef]
12. Ang, H.M.; Reyhani, M.; Tad, M.O.; Safaeefar, P. Growth Kinetics of Manganese Sulphate from Heating and Salting-out Batch Crystallisation. *Dev. Chem. Eng. Miner. Process.* **2006**, *14*, 303–312. [CrossRef]
13. Li, X.; Ji, D.; Su, H.; Pan, L.; Li, J.; Li, J.; Wen, Y. Study on production of manganese sulphate by high-temperature crystallizing process. *Inorg. Chem. Ind.* **2010**, *42*, 16–19. [CrossRef]
14. Zhao, J.; Wang, W.; Cao, J.; Kou, X. Purification of calcium and magnesium from industrial manganese sulfate liquid by fluoride precipitant. *Ind. Water Treat.* **2019**, *39*, 77–81. [CrossRef]
15. Wang, Y.; Zeng, L.; Zhang, G.; Guan, W.; Sun, Z.; Zhang, D.; Qing, J. A novel process on separation of manganese from calcium and magnesium using synergistic solvent extraction system. *Hydrometallurgy* **2019**, *185*, 55–60. [CrossRef]
16. Dan, D.; Liu, Z.; Sun, L.; Tang, L.; Zou, X. Removal of Ca and Mg Ions from Industrial Manganese Sulfate Solution by Solvent Extraction. *J. Jishou Univ.* **2016**, *37*, 55–62. [CrossRef]
17. Liu, H.; Zhu, G. Study on removal of calcium and magnesium from Leaching solution of manganese ore by solvent extraction. *China's Manganese Ind.* **2008**, *26*, 34–37. [CrossRef]
18. Ilea, P.; Popescu, I.C.; Urdă, M.; Oniciu, L. The electrodeposition of manganese from aqueous solutions of $MnSO_4$. IV: Electrowinning by galvanostatic electrolysis. *Hydrometallurgy* **1997**, *46*, 149–156. [CrossRef]
19. Farrah, H.E.; Lawrance, G.A.; Wanless, E.J. Solubility of calcium sulfate salts in acidic manganese sulfate solutions from 30 to 105°C. *Hydrometallurgy* **2007**, *86*, 13–21. [CrossRef]
20. He, Y.; Li, F.; Luo, Z.; Luo, K. Preparation of Battery-Grade Manganese Sulfate by Purification of Industrial-Grade Manganese Sulfate with High-Temperature Crystallization Method. *Min. Metall. Eng.* **2019**, *39*, 85–88. [CrossRef]
21. Yuan, F.; Feng, Y.; Li, H.; Yi, A.; Li, H.; Wu, M.; Guo, C. Research on Separation of Manganese and Manganese From Manganese Sulfate Solution Containing Magnesium by Evaporation Crystallization. *Hydrometall. China* **2015**, *34*, 225–228. [CrossRef]
22. Giulietti, M.; Seckler, M.M.; Derenzo, S.; Ré, M.I.; Cekinski, E. Industrial Crystallization and Precipitation from Solutions: State of the Technique. *Braz. J. Chem. Eng.* **2001**, *18*, 423–440. [CrossRef]
23. Zou, X. Present Situation of Production Technology of High Purity Manganese Sulfate. *China's Manganese Ind.* **2018**, *36*, 4–6. [CrossRef]
24. Jakovljevic, B.; Bourget, C.; Nucciarone, D. CYANEX (R) 301 binary extractant systems in cobalt/nickel recovery from acidic chloride solutions. *Hydrometallurgy* **2004**, *75*, 25–36. [CrossRef]
25. Pakarinen, J.; Paatero, E. Effect of temperature on Mn-Ca selectivity with organophosphorus acid extractants. *Hydrometallurgy* **2011**, *106*, 159–164. [CrossRef]
26. Benrath, V.A.; Blankenstein, A. Uber mischkristalle in der vitriolreihe I. *Z. Furanorgaische Und All Gem. Chem Emio* **1933**, *216*, 41–47. [CrossRef]
27. Yang, S.; Ren, B.; Wang, C. The Study of Magnesium Removing by Ethanol Recycling for the Technology of Electrolytic Manganese Processing. *China's Manganese Ind.* **2011**, *29*, 15–17. [CrossRef]
28. Li, W.; Jia, J.; Zhao, X.; Ji, Y. Simulation and analysis of produced water in Anhui oil production plant with software OLI ANALYZER STUDIO. *Comput. Appl. Chem.* **2013**, *30*, 179–182. [CrossRef]
29. Liu, J.; Wu, J.; Feng, J.; Yan, W. A Review of Fabrication and Purification of Manganese Sulphate. *China's Manganese Ind.* **2017**, *35*, 114–118. [CrossRef]
30. Yuan, M.; Qiu, G. Study on the removing of $MgSO_4$ from $MnSO_4$ solution based on the aqueous system phase diagram. *Cent. South Univ. Technol.* **2000**, 212–214. [CrossRef]
31. Cottrell, F.G. On the Solubility of Manganous Sulphate. *J. Phys. Chem.* **2002**, *4*, 637–656. [CrossRef]
32. Matricardi, L.R.; Downing, J.; Staff, U.B. Manganese and Manganese Alloys. *Kirk-Othmer Encycl. Chem. Technol.* **2012**. [CrossRef]
33. Safaeefar, P.; Ang, H.M.; Kuramochi, H.; Asakuma, Y.; Maeda, K.; Tade, M.O.; Fukui, K. Measurement and correlation of the solubility of $MnSO_4 \cdot H_2O$ in ethanol+water+$MgSO_4 \cdot 7H_2O$ solutions. *Fluid Phase Equilibria* **2006**, *250*, 64–69. [CrossRef]